

## Electronic Supplementary Information (ESI)

# In-situ Growth of Crystalline Carbon Nitride on LaOCl for Photocatalytic Overall Water Splitting

*Yuan Lin, Xuxu Wang, Xianzhi Fu, Wenyue Su\**

*State Key Laboratory of Photocatalysis on Energy and Environment, College of Chemistry,  
Fuzhou University, Fuzhou, 350116, PR China*

\*Corresponding author. E-mail: suweny@fzu.edu.cn

### Contents list

#### Experimental Section

- Figure S1.** Schematic of two-step photon excitation (a) and one-step photon excitation (b) pathway.
- Figure S2.** SEM images of LaOCl (a) and CCN (b).
- Figure S3.** HRTEM image of PCN/LaOCl (a) and CCN/LaOCl (b).
- Figure S4.** Nitrogen adsorption–desorption isotherms of CCN, CCN/LaOCl-*x* and PCN/LaOCl.
- Figure S5.** SEM image of (a) CCN/LaOCl-1.5 and (b) CCN/LaOCl-2.
- Figure S6.** UV/Vis DRS spectrum of CCN, CCN/LaOCl-*x* and LaOCl.
- Figure S7.** High resolution XPS spectra of (a) C 1s and (b) N 1s of CCN/LaOCl and CCN. (c) High resolution XPS spectra of La 3d for LaOCl and CCN/LaOCl.
- Figure S8.** The transient photocurrents of the prepared electrodes covered with PCN/LaOCl and CCN/LaOCl.
- Figure S9.** The EIS Nyquist plots of the prepared electrodes covered with PCN/LaOCl and CCN/LaOCl.
- Figure S10.** Photoluminescence spectra of PCN/LaOCl and CCN/LaOCl with excitation wavelength of 363 nm.
- Figure S11.** XRD patterns of CCN/LaOCl before and after the photocatalytic reaction.
- Figure S12.** XPS survey spectrum (a), High resolution XPS spectra of C 1s (b), N 1s (c), La 3d (d), O 1s (e), Cl 2p (f), Pt 4f (g) and Co 2p (h) for Pt, CoO<sub>x</sub> loaded CCN/LaOCl before and after the photocatalytic reaction.
- Figure S13.** UPS spectra of CCN (a) and LaOCl (b).
- Figure S14.** Tauc plots of CCN (a) and LaOCl (b).

**Figure S15.** (a) HRTEM images of the CCN/LaOCl sample after the deposition of Pt. The corresponding EDS spectra (inset) indicates that there is a signal of Pt.

**Figure S16.** (a) HRTEM image of the CCN/LaOCl sample after the deposition of  $\text{CoO}_x$ , the image showing two variant shapes, among which the sheet-like one corresponds to CCN matrix, this is verified by the EDS mapping as displayed in the inset of (a). (b) EDS-HAADF image of the CCN/LaOCl sample after the deposition of  $\text{CoO}_x$ , the line profile across the nanoparticle in the inset of (b) demonstrates that the bright contrast corresponds to  $\text{CoO}_x$  particles.

**Table S1.** The BET specific surface area and the CCN amount of CCN/LaOCl-x samples.

**Table S2.** Fs-TA exponential function fitted parameters of absorption decay for PCN/LaOCl and CCN/LaOCl at 650 nm.

**Table S3.** Exponential function fitted parameters of the time-resolved PL decay spectra for the prepared samples.

**Table S4.** Comparison of photocatalytic activity for overall water splitting over carbon nitride-based materials.

**Table S5.** AQE of CCN/LaOCl for overall water splitting.

## Experimental Section

**Characterization of materials:** Scanning electron microscopy (SEM) images were collected using a Hitachi SU8010 field emission scanning electron microscope. Transmission electron microscopy (TEM) was performed using a Talos F200S microscope. The powder X-ray diffraction (XRD) was analyzed using a Bruker D8 Advance X-ray diffractometer. Solid-state  $^{13}\text{C}$  NMR measurements were performed on a Bruker Advance 500 spectrometer. Electron paramagnetic resonance (EPR) spectra was recorded on a Bruker A300 spectrometer. UV-vis diffuse reflectance spectra (UV-vis DRS) were obtained using a Varian Cary 5000 Scan UV-vis-NIR spectrophotometer. The Brunauer–Emmett–Teller (BET) specific surface areas were measured with an ASAP 2020 (Micromeritics Instrument Corp.). The contents of C and N are determined by element analysis (Vario EL Cube). X-ray photoelectron spectroscopy (XPS) measurements were performed on an ESCALAB 250 photoelectron spectroscopy system with the C1s peak (284.6 eV) as a reference. Ultraviolet photoelectron spectroscopy (UPS) measurements were conducted using an unfiltered He I (21.22 eV) gas discharge lamp. Femtosecond Transient Absorption (fsTA) measurements were performed through a femtosecond Ti:Sapphire regenerative amplified laser system (Spectra Physics, Spitfire-Pro) and the corresponding data acquisition system (Ultrafast Systems, Helios model), samples were irradiated with 400 nm laser light, and the data were collected by the acquisition system as the three-dimensional wavelength-time-absorbance matrices that were exported for further use with the fitting software. Photoluminescence (PL) spectra were obtained with an F-7000 FL spectrophotometer. The electrochemical impedance spectra (EIS) and photocurrent-time (I-t) profiles were conducted on a CHI660D electrochemical workstation using a Pt plate as the counter electrode and a saturated calomel electrode as the reference electrode, respectively. A 0.2 M  $\text{Na}_2\text{SO}_4$  solution was used as the electrolyte. To fabricate the working electrode, 20 mg sample was dispersed in 1 mL dimethylformamide (DMF) solvent with 40  $\mu\text{L}$  Nafion solution (5 wt.%, Du Pont) to form a homogeneous ink with ultra-sonication for 30 min. Next, 15  $\mu\text{L}$  of the dispersion was loaded onto fluorine-doped tin oxide (FTO) glass with an area of 0.25  $\text{cm}^2$  as the working electrode. The work functions (WF) of CCN and LaOCl were determined by Kelvin probe system (SKP5050, KP Technology Ltd.) with a single-point measurement. The work function of the tip was corrected using a gold disk (gold, 5.1 eV). The relationship between the (work functions) WF and the contact potential difference (CPD) can be calculated on the followed formula:

$$WF_{\text{sample}} = WF_{\text{tip}} + \text{CPD}$$

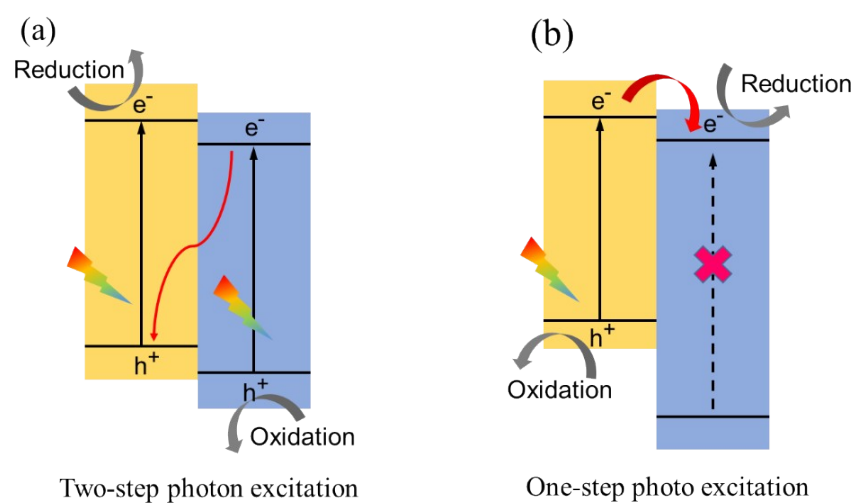


**Figure S1.** Schematic of two-step photon excitation (a) and one-step photon excitation (b) pathway.

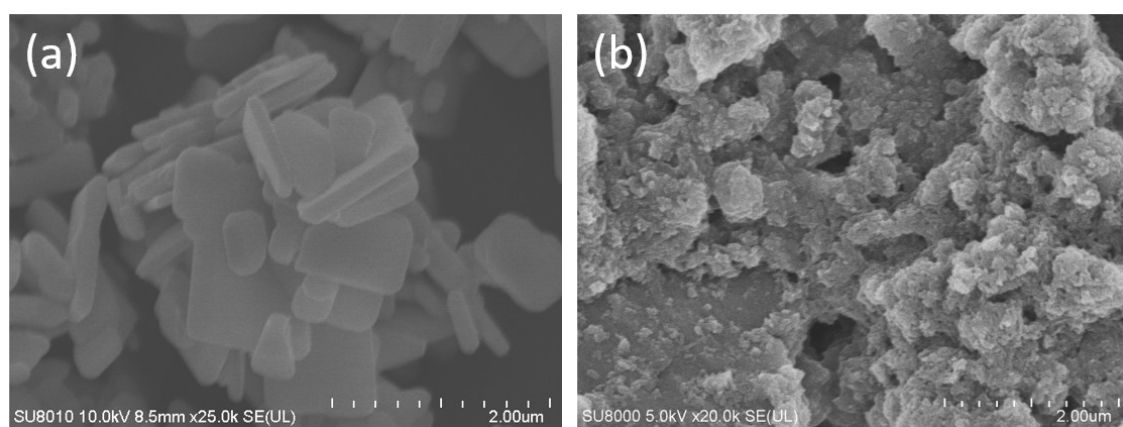


**Figure S2.** SEM images of LaOCl (a) and CCN (b).

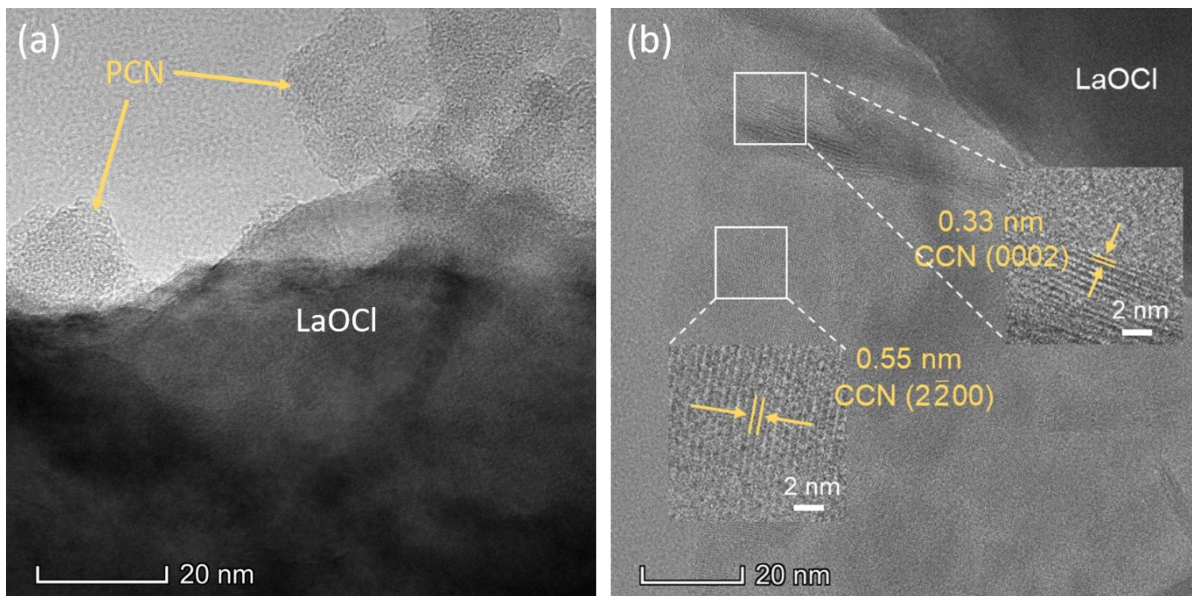


**Figure S3.** HRTEM image of PCN/LaOCl (a) and CCN/LaOCl (b).

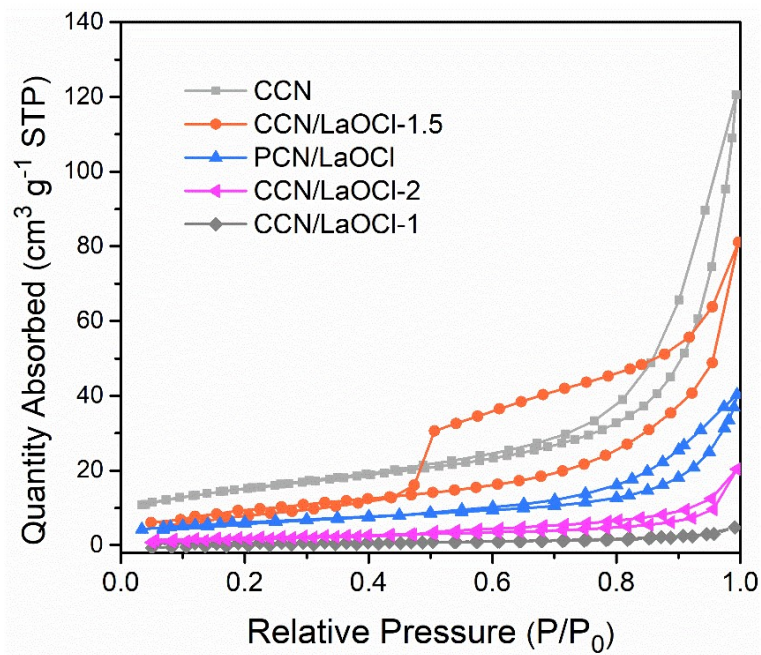


**Figure S4.** Nitrogen adsorption–desorption isotherms of CCN, CCN/LaOCl-*x* and PCN/LaOCl.

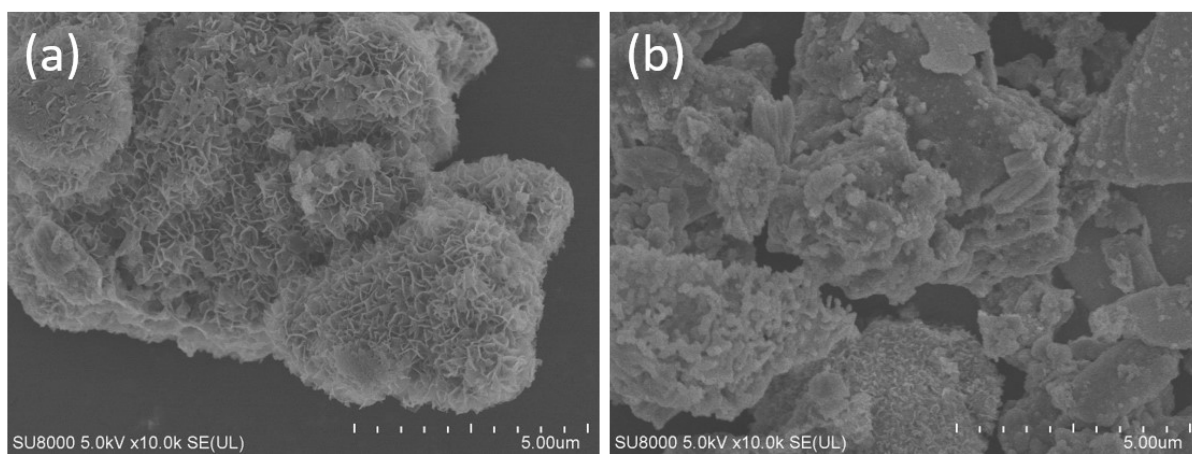


**Figure S5.** SEM image of (a) CCN/LaOCl-1.5 and (b) CCN/LaOCl-2.

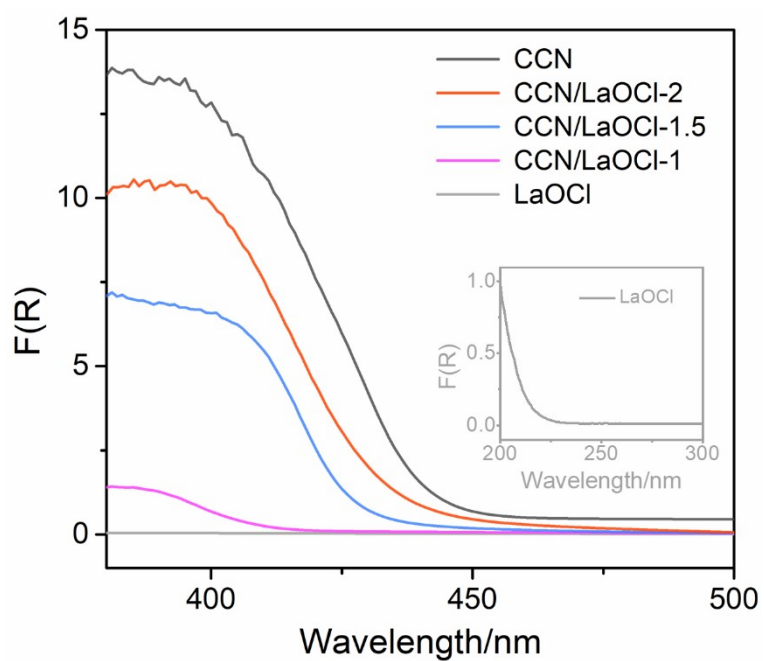


**Figure S6.** UV/Vis DRS spectrum of CCN, CCN/LaOCl- $x$  and LaOCl.



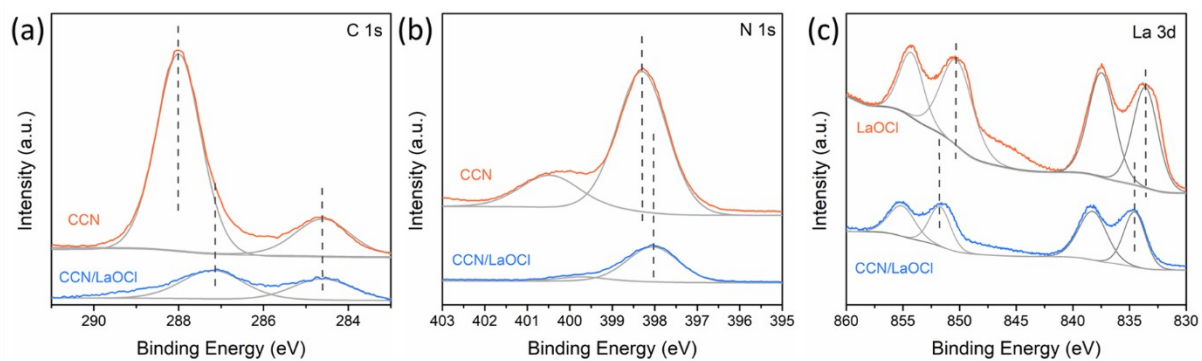


**Figure S7.** High resolution XPS spectra of (a) C 1s and (b) N 1s of CCN/LaOCl and CCN. (c) High resolution XPS spectra of La 3d for LaOCl and CCN/LaOCl.

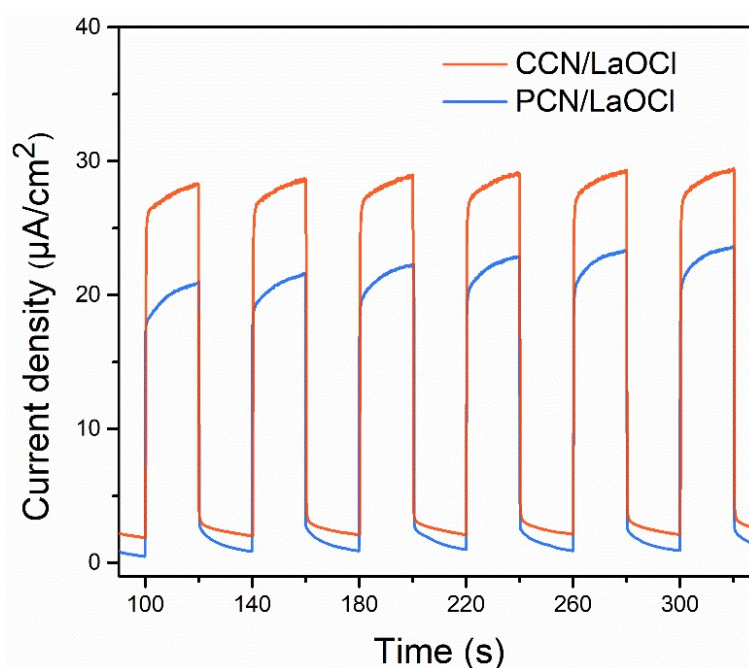


**Figure S8.** The transient photocurrents of the prepared electrodes covered with PCN/LaOCl and CCN/LaOCl.

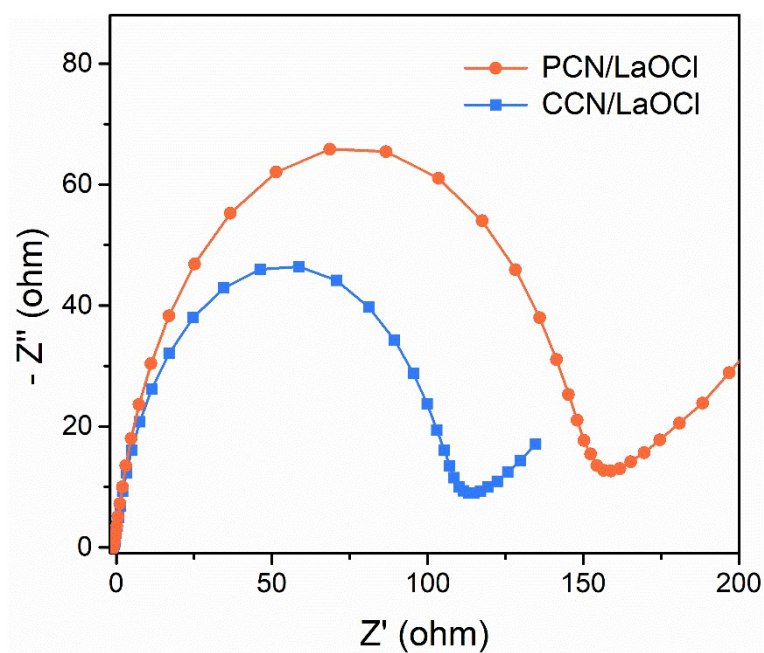


**Figure S9.** The EIS Nyquist plots of the prepared electrodes covered with PCN/LaOCl and CCN/LaOCl.

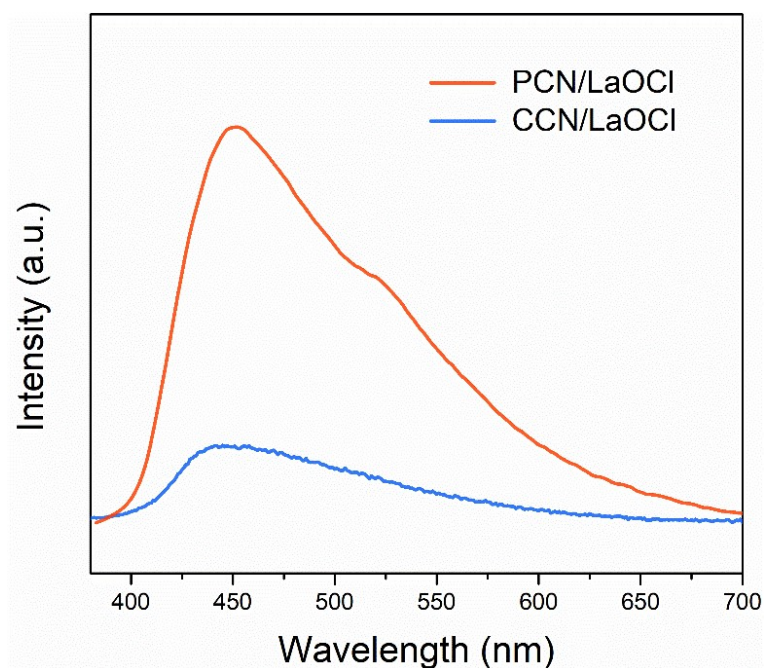


**Figure S10.** Photoluminescence spectra of PCN/LaOCl and CCN/LaOCl with excitation wavelength of 363 nm.



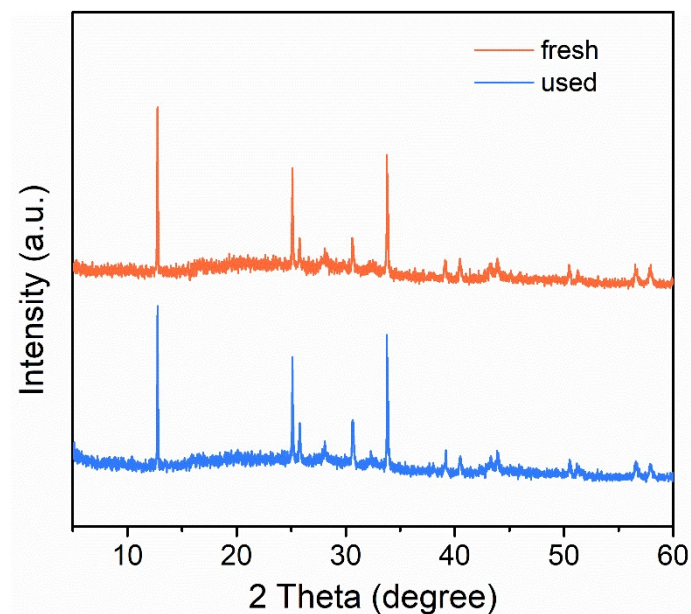


**Figure S11.** XRD patterns of CCN/LaOCl before and after the photocatalytic reaction.

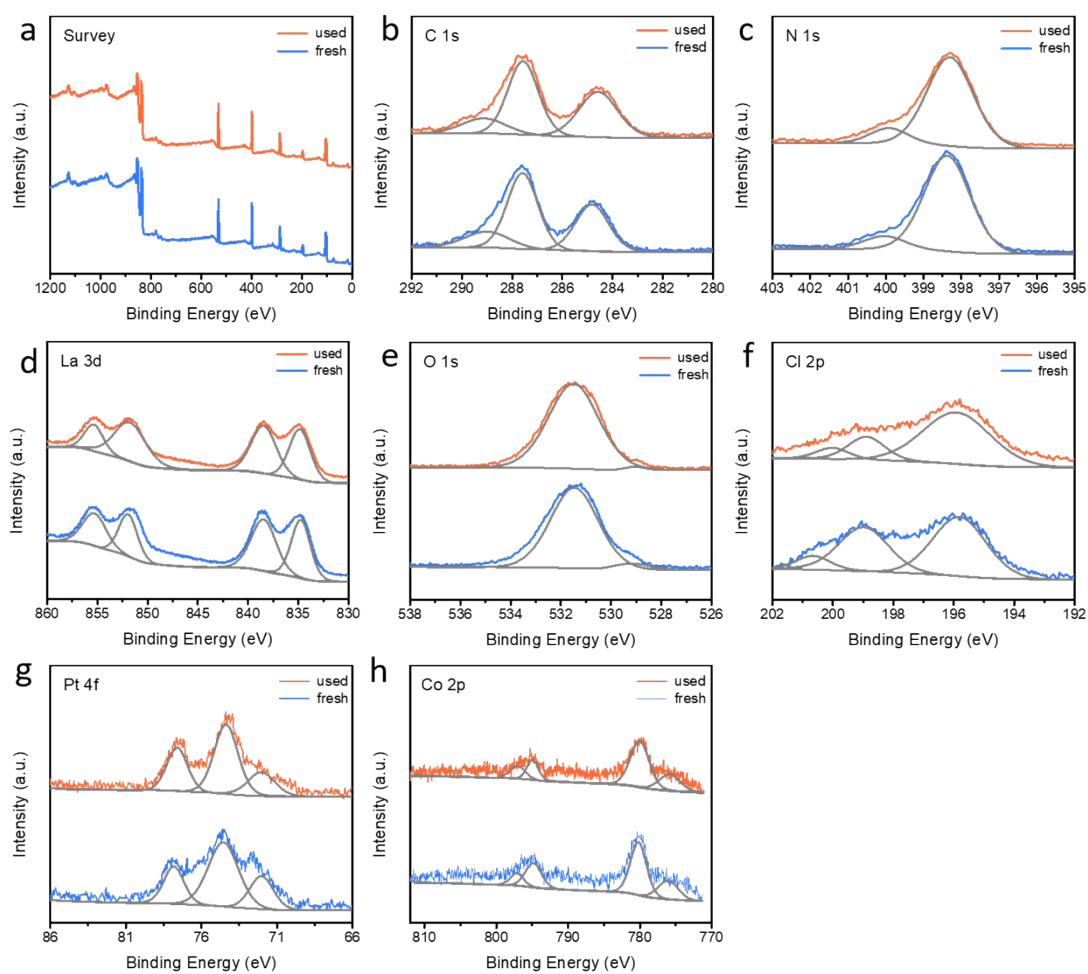


**Figure S12.** XPS survey spectrum (a), High resolution XPS spectra of C 1s (b), N 1s (c), La 3d (d), O 1s (e), Cl 2p (f), Pt 4f (g) and Co 2p (h) for Pt, CoO<sub>x</sub> loaded CCN/LaOCl before and after the photocatalytic reaction.

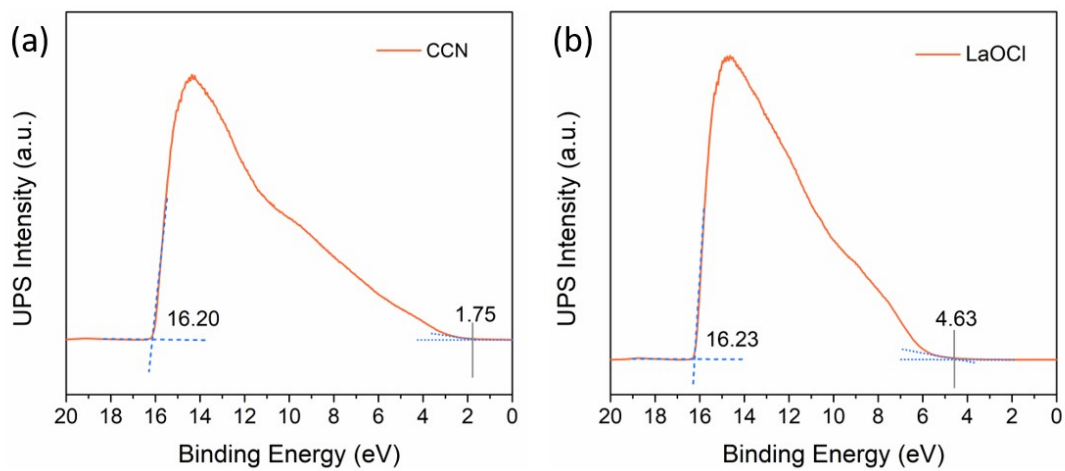


**Figure S13.** UPS spectra of CCN (a) and LaOCl (b).

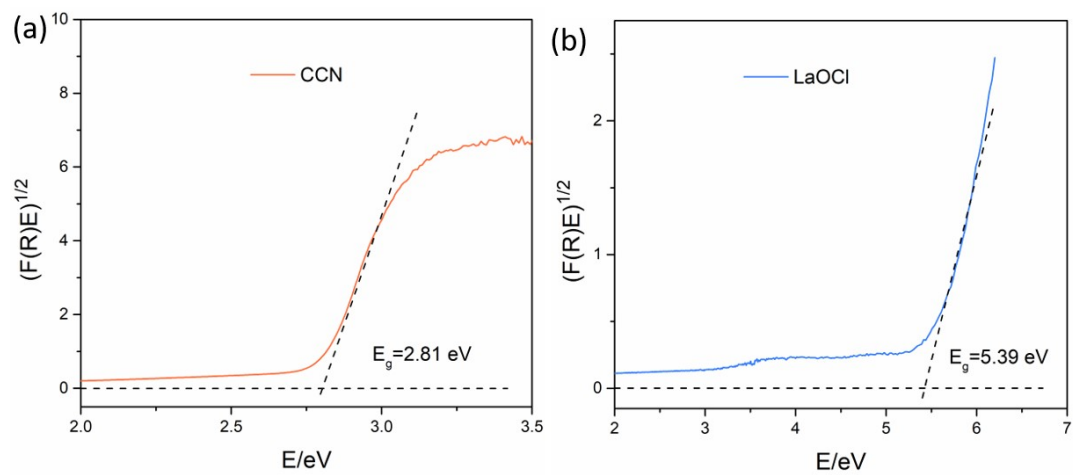


**Figure S14.** Tauc plots of CCN (a) and LaOCl (b).

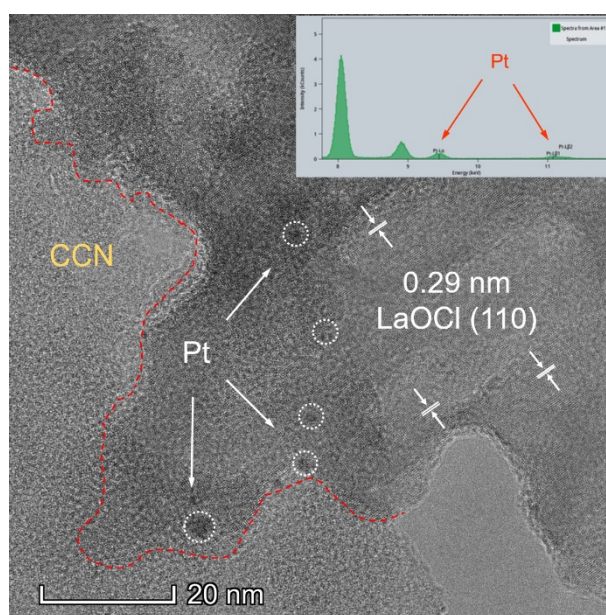


**Figure S15.** (a) HRTEM images of the CCN/LaOCl sample after the deposition of Pt. The corresponding EDS spectra (inset) indicates that there is a signal of Pt.

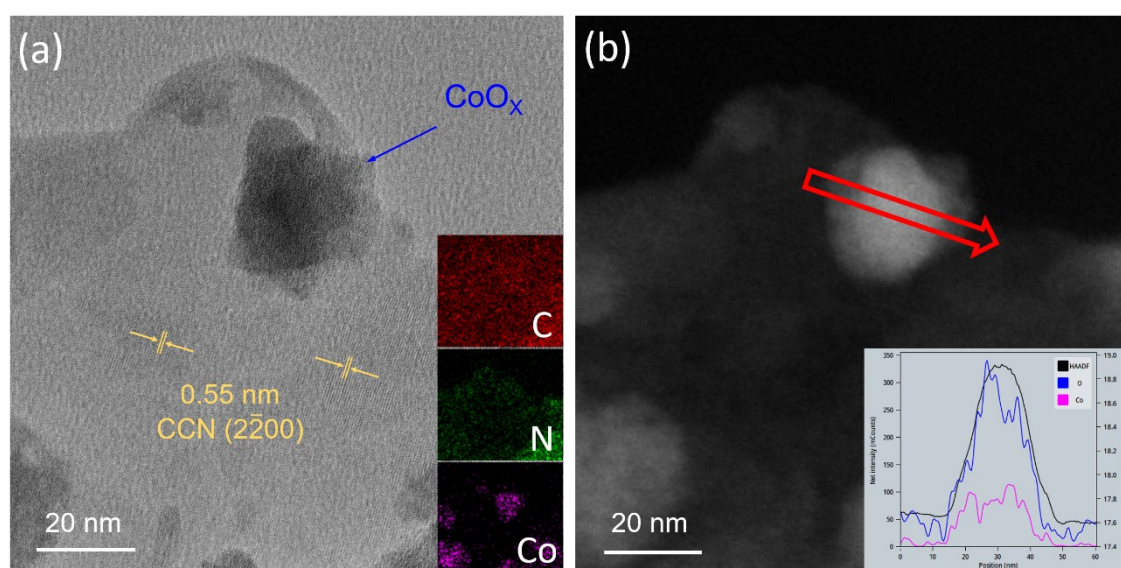


**Figure S16.** (a) HRTEM image of the CCN/LaOCl sample after the deposition of  $\text{CoO}_x$ , the image showing two variant shapes, among which the sheet-like one corresponds to CCN matrix, this is verified by the EDS mapping as displayed in the inset of (a). (b) EDS-HAADF image of the CCN/LaOCl sample after the deposition of  $\text{CoO}_x$ , the line profile across the nanoparticle in the inset of (b) demonstrates that the bright contrast corresponds to  $\text{CoO}_x$  particles.

**Table S1.** The BET specific surface area and the CCN amount of CCN/LaOCl-x samples.

Samples	Specific surface area (m <sup>2</sup> /g)	wt. % of CCN
LaOCl	3.8	-
CCN/LaOCl-0.5	4.0	5.7
CCN/LaOCl-1	4.3	13.1
CCN/LaOCl-1.5	34.3	30.9
CCN/LaOCl-2	8.6	40.4
CCN/LaOCl-3	8.1	45.7

**Table S2.** Fs-TA exponential function fitted parameters of absorption decay for PCN/LaOCl and CCN/LaOCl at 650 nm.

Materisla	$\tau_1$ (ps)	A <sub>1</sub> (%)	$\tau_2$ (ps)	A <sub>2</sub> (%)	Average $\tau$ (ps)
PCN/LaOCl	12.9	55.4	158	44.6	77.6
CCN/LaOCl	13.5	58.2	224	41.8	101.4

**Table S3.** Exponential function fitted parameters of the time-resolved PL decay spectra for the prepared samples.

Samples	$\tau_1$ (ns)	A <sub>1</sub> (%)	$\tau_2$ (ns)	A <sub>2</sub> (%)	Average $\tau$ (ns)
PCN/LaOCl	3.30	16	0.61	84	1.03
CCN/LaOCl	4.16	39	0.79	61	2.12

**Table S4.** Comparison of photocatalytic activity for overall water splitting over carbon nitride-based materials.

Materials	Reaction conditions	H <sub>2</sub> evolution rate (μmol h <sup>-1</sup> )	O <sub>2</sub> evolution rate (μmol h <sup>-1</sup> )	AQE (%)	Ref.
CCN/LaOCl	300 W Xe lamp, 50 mg catalyst, 0.5 wt.% Pt, 0.2 wt.% CoO <sub>x</sub> cocatalyst	60.6 (λ > 300 nm) 20.2 (λ > 400 nm)	28.1 (λ > 300 nm) 9.1 (λ > 400 nm)	1.13 (400 nm)	<b>This work</b>
PCN/LaOCl	300 W Xe lamp, 50 mg catalyst, 0.5 wt.% Pt, 0.2 wt.% CoO <sub>x</sub> cocatalyst	22.3 (λ > 300 nm) 8 (λ > 400 nm)	10.7 (λ > 300 nm) 3.8 (λ > 400 nm)	0.33 (400 nm)	[1]
g-C <sub>3</sub> N <sub>4</sub> /rGO/PDIP	300 W Xe lamp, 25 mg catalyst, Pt/Cr <sub>2</sub> O <sub>3</sub> , Co(OH) <sub>2</sub> cocatalyst	15.8 (λ > 420 nm)	7.8 (λ > 420 nm)	3.6 (420 nm)	[2]
CNN/BDCNN	300 W Xe lamp, 40 mg catalyst, 0.9 wt.% Pt and 3.0 wt.% Co(OH) <sub>2</sub> cocatalyst	32.9 (λ > 300 nm) 9.85 (λ > 420 nm)	16.4 (λ > 300 nm) 4.88 (λ > 420 nm)	11.90 (400 nm)	[3]
BDCNN350/B DCNN425	300 W Xe lamp, 100 mg catalyst, 0.9 wt.% Pt and 3.0 wt.% Co(OH) <sub>2</sub> cocatalyst	62.9 (λ > 300 nm)	31.3 (λ > 300 nm)	23.52 (420 nm)	[3]
PTI-550	300 W Xe lamp, 100 mg catalyst, 0.5 wt.% Co and 1.0 wt.% Pt cocatalyst	189 (λ > 300 nm)	91 (λ > 300 nm)	8 (365 nm)	[4]
3D g-C <sub>3</sub> N <sub>4</sub> NS	300 W Xe lamp, 50 mg catalyst, 1 wt.% Pt, 3 wt.% IrO <sub>2</sub> cocatalyst	5.1 (λ > 420 nm)	2.5 (λ > 420 nm)	1.4 (420 nm)	[5]
Fe <sub>2</sub> O <sub>3</sub> /RGO/PCN	300 W Xe lamp, 40 mg catalyst, Pt cocatalyst	43.6 (λ > 300 nm) 6 (λ > 400 nm)	21.2 (λ > 300 nm) 3 (λ > 400 nm)	N/A	[6]
Pt/g-C <sub>3</sub> N <sub>4</sub>	300 W Xe lamp, 200 mg catalyst, 3 wt.% Pt, 1 wt.% CoO <sub>x</sub> cocatalyst	12.2 (λ > 300 nm) 1.2 (λ > 420 nm)	6.3 (λ > 400 nm) 0.6 (λ > 420 nm)	0.3 (405 nm)	[7]
Co <sub>3</sub> O <sub>4</sub> /HCNS/Pt	300 W Xe lamp, 20 mg catalyst, 1 wt.% Pt, 3 wt.% Co <sub>3</sub> O <sub>4</sub> cocatalyst	3.2 (λ > 300 nm)	1.7 (λ > 300 nm)	N/A	[8]
Pt/CoP/g-C <sub>3</sub> N <sub>4</sub>	300 W Xe lamp, 80 mg catalyst, pH = 3, 3 wt.% Pt, 3 wt.% CoP cocatalyst	21 (λ > 300 nm) 2.1 (λ > 400 nm)	10 (λ > 300 nm) 1.0 (λ > 400 nm)	N/A	[9]
α-Fe <sub>2</sub> O <sub>3</sub> /2D-C <sub>3</sub> N <sub>4</sub>	300 W Xe lamp, 10 mg catalyst, 3 wt.% Pt, 0.1 wt.% RuO <sub>2</sub> cocatalyst	0.38 (λ > 400 nm)	0.19 (λ > 400 nm)	N/A	[10]
Na-CN	300 W Xe lamp, 100 mg catalyst, 1 wt.% Pt cocatalyst	31.5 (λ > 420 nm)	15.2 (λ > 420 nm)	1.45 (420 nm)	[11]
Co <sub>1</sub> -phosphide/CN	300 W Xe lamp, 20 mg catalyst,	8.2 (λ > 300 nm) 2,5 (λ > 420 nm)	4.1 (λ > 300 nm) 1.3 (λ > 420 nm)	2.2 (500 nm)	[12]
(C <sub>ring</sub> )-C <sub>3</sub> N <sub>4</sub>	300 W Xe lamp, 30 mg catalyst, 3 wt.% of Pt cocatalyst	11.1 (λ > 300 nm) 4.5 (λ > 420 nm)	5.5 (λ > 300 nm) 2.2 (λ > 420 nm)	5 (420 nm)	[13]
C <sub>Co</sub> -C <sub>3</sub> N <sub>4</sub>	300 W Xe lamp, 30 mg catalyst,	15.9 (λ > 300 nm)	7.7 (λ > 300 nm)	N/A	[14]
CQDs/ holey CN	300 W Xe lamp, 10 mg catalyst, 2 wt.% of Pt cocatalyst	9.3 (λ > 420 nm)	4.6 (λ > 420 nm)	N/A	[15]

CoO/g-C <sub>3</sub> N <sub>4</sub>	LED, 50 mg catalyst,	2.5 ( $\lambda > 400$ nm)	1.4 ( $\lambda > 400$ nm)	1.91 (420 nm)	[16]
C <sub>3</sub> N <sub>4</sub> /MnO <sub>2</sub>	300 W Xe lamp, 100 mg catalyst,	5.5 ( $\lambda > 420$ nm)	2.8 ( $\lambda > 420$ nm)	~3.7 (420 nm)	[17]
g-C <sub>3</sub> N <sub>4</sub> -carbon dots	300 W Xe lamp, 100 mg catalyst,	0.5 ( $\lambda > 420$ nm)	0.25 ( $\lambda > 420$ nm)	N/A	[18]
MnO <sub>2</sub> /g-C <sub>3</sub> N <sub>4</sub>	300 W Xe lamp, 100 mg catalyst, 3 wt.% of Pt cocatalyst	6.1 ( $\lambda > 400$ nm)	2.9 ( $\lambda > 400$ nm)	N/A	[19]
Mn-C <sub>3</sub> N <sub>4</sub>	300 W Xe lamp, 20 mg catalyst, 0.9 wt.% of Pt cocatalyst	13.9 ( $\lambda > 300$ nm) 6.1 ( $\lambda > 420$ nm)	6.6 ( $\lambda > 300$ nm) 2.9 ( $\lambda > 420$ nm)	4.0 (420 nm)	[20]
TH-CN	300 W Xe lamp, 50 mg catalyst, 1 wt. % CoP, 1.5 wt. % Pt, Ph=5.6	10.2 ( $\lambda > 400$ nm)	5.7 ( $\lambda > 400$ nm)	N/A	[21]
PTI-LiNa	300 W Xe lamp, 100 mg catalyst, 0.5 wt% Co and 1.0 wt% Pt cocatalyst	273 ( $\lambda > 300$ nm)	135 ( $\lambda > 300$ nm)	12% (365 nm)	[22]
NdCo <sub>3</sub> /PCN	300 W Xe lamp, 40 mg catalyst	11.8 ( $\lambda > 300$ nm) 0.7 ( $\lambda > 420$ nm)	6.0 ( $\lambda > 300$ nm) 0.35 ( $\lambda > 420$ nm)	2.0 (350 nm)	[23]
C <sub>3</sub> N <sub>4</sub> -Cl4	20 mg catalyst, Pt cocatalyst	48.2 ( $\lambda > 300$ nm)	21.8 ( $\lambda > 300$ nm)	6.9 (420 nm)	[24]

**Table S5.** AQE of CCN/LaOCl for overall water splitting.

Wavelengths (nm)	H <sub>2</sub> evolution ( $\mu\text{mol/h}$ )	Light power (mW/cm <sup>2</sup> )	irradiated area (cm <sup>2</sup> )	AQE(%)
380	31.4	13.42	32.15	1.27
400	37.6	17.16	32.15	1.13
420	11.2	12.53	32.15	0.44
450	2.1	17.06	32.15	0.05
475	0.6	16.11	32.15	0.02

## References for Supporting Information

- [1] Y. Lin, W. Su, X. Wang, X. Fu, X. Wang, *Angew. Chem. Int. Ed.* 2020, 59, 20919.  
[2] X. Chen, J. Wang, Y. Chai, Z. Zhang, Y. Zhu, *Adv. Mater.* 2021, 33, e2007479.  
[3] D. Zhao, Y. Wang, C.-L. Dong, Y.-C. Huang, J. Chen, F. Xue, S. Shen, L. Guo, *Nat. Energy* 2021, 6, 388.  
[4] L. H. Lin, Z. Y. Lin, J. Zhang, X. Cai, W. Lin, Z. Y. Yu, X. C. Wang, *Nat. Catal.* 2020, 3, 649.  
[5] X. Chen, R. Shi, Q. Chen, Z. Zhang, W. Jiang, Y. Zhu, T. Zhang, *Nano Energy* 2019, 59, 644.  
[6] Z. Pan, G. Zhang, X. Wang, *Angew. Chem. Int. Ed.* 2019, 58, 7102.  
[7] G. Zhang, Z. A. Lan, L. Lin, S. Lin, X. Wang, *Chem. Sci.* 2016, 7, 3062.  
[8] D. Zheng, X. N. Cao, X. Wang, *Angew. Chem. Int. Ed.* 2016, 55, 11512.



- [9] Z. Pan, Y. Zheng, F. Guo, P. Niu, X. Wang, *ChemSusChem* 2017, 10, 87.
- [10] X. She, J. Wu, H. Xu, J. Zhong, Y. Wang, Y. Song, K. Nie, Y. Liu, Y. Yang, M.-T. F. Rodrigues, R. Vajtai, J. Lou, D. Du, H. Li, P. M. Ajayan, *Adv. Energy Mater.* 2017, 7, 1700025.
- [11] F. Guo, J. Chen, M. Zhang, B. Gao, B. Lin, Y. Chen, *J. Mater. Chem. A* 2016, 4, 10806.
- [12] W. Liu, L. Cao, W. Cheng, Y. Cao, X. Liu, W. Zhang, X. Mou, L. Jin, X. Zheng, W. Che, Q. Liu, T. Yao, S. Wei, *Angew. Chem. Int. Ed.* 2017, 56, 9312.
- [13] W. Che, W. Cheng, T. Yao, F. Tang, W. Liu, H. Su, Y. Huang, Q. Liu, J. Liu, F. Hu, Z. Pan, Z. Sun, S. Wei, *J. Am. Chem. Soc.* 2017, 139, 3021.
- [14] X. Fang, R. Gao, Y. Yang, D. Yan, *iScience* 2019, 16, 22.
- [15] T. Song, P. Zhang, T. Wang, A. Ali, H. Zeng, *Appl. Catal. B-Environ.* 2018, 224, 877.
- [16] F. Guo, W. Shi, C. Zhu, H. Li, Z. Kang, *Appl. Catal. B-Environ.* 2018, 226, 412.
- [17] J. Liu, N. Y. Liu, H. Li, L. P. Wang, X. Q. Wu, H. Huang, Y. Liu, F. Bao, Y. Lifshitz, S. T. Lee, Z. H. Kang, *Nanoscale* 2016, 8, 11956.
- [18] D. Qu, J. Liu, X. Miao, M. Han, H. Zhang, Z. Cui, S. Sun, Z. Kang, H. Fan, Z. Sun, *Appl. Catal. B-Environ.* 2018, 227, 418.
- [19] Z. Mo, H. Xu, Z. Chen, X. She, Y. Song, J. Lian, X. Zhu, P. Yan, Y. Lei, S. Yuan, H. Li, *Appl. Catal. B-Environ.* 2019, 241, 452.
- [20] S. Sun, G. Shen, J. Jiang, W. Mi, X. Liu, L. Pan, X. Zhang, J. J. Zou, *Adv. Energy Mater.* 2019, 1901505.
- [21] Z. Pan, M. Liu, G. Zhang, H. Zhuzhang, X. Wang, *J. Phys. Chem. C* 2021, 125, 9818.
- [22] M. Liu, C. Wei, H. Zhuzhang, J. Zhou, Z. Pan, W. Lin, Z. Yu, G. Zhang, X. Wang, *Angew. Chem. Int. Ed.* 2022, 61, e202113389.
- [23] R. Chen, G. L. Zhuang, Z. Y. Wang, Y. J. Gao, Z. Li, C. Wang, Y. Zhou, M. H. Du, S. Zeng, L. S. Long, X. J. Kong, L. S. Zheng, *Natl. Sci. Rev.* 2021, 8, nwaa234.
- [24] Q. Zhang, X. Chen, Z. Yang, T. Yu, L. Liu, J. Ye, *ACS Appl. Mater. Interfaces* 2022, 14, 3970.